The Effect of Carbon Nanotube on the Physical Properties of Poly(butylene terephthalate) Nanocomposite by Simple Melt Blending

Jun Young Kim[1,2]

[1]*Material Laboratory, Corporate R&D Center, Samsung SDI Co., Ltd., Suwon-si, Gyeonggi-do 443-731, Republic of Korea*
[2]*Department of Materials Science and Engineering, Massachusetts Institute of Technology, Cambridge, Massachusetts 02139, USA*

Received 18 August 2008; accepted 19 October 2008
DOI 10.1002/app.29560
Published online 19 February 2009 in Wiley InterScience (www.interscience.wiley.com).

ABSTRACT: Polyester nanocomposites based on poly(butylene terephthalate) (PBT) and carbon nanotube (CNT) were prepared by simple melt blending using a twin-screw extruder. There is significant dependence of the thermal, rheological, and mechanical properties of the PBT nanocomposites on the concentration and dispersion state of CNT. The storage and loss moduli of the PBT nanocomposites increased with increasing frequency, and this enhancing effect was more pronounced at lower frequency region. The nonterminal behavior for the PBT nanocomposites was attributed to the nanotube–nanotube or polymer–nanotube interactions, and the dominant nanotube–nanotube interactions at high CNT content resulted in the formation of the interconnected network-like structures of CNT in the PBT nanocomposites. The incorporation of a small quantity of CNT into the PBT matrix can substantially improve the mechanical properties, the heat distortion temperature, and the thermal stability of the PBT nanocomposites. The unique character of CNT dispersed in the PBT matrix resulted in the physical barrier effect against the thermal decomposition, leading to the improvement in the thermal stability of the PBT nanocomposites. This study also provides a design guide of CNT-reinforced PBT nanocomposites with a great potential for industrial uses. © 2009 Wiley Periodicals, Inc. J Appl Polym Sci 112: 2589–2600, 2009

Key words: blending; carbon nanotube; nanocomposites; poly(butylene terephthalate); reinforcement

INTRODUCTION

During the rapid advancement in the materials science and technology, much research has extensively undertaken on high-performance polymer composites for targeted applications in numerous industrial fields. Furthermore, a great number of efforts have been made to develop high-performance polymer nanocomposites with the benefit of nanotechnology.[1–3] These attempts include studies of polymer composites with the introduction of nanoscaled reinforcing fillers into the polymer matrix.[1–5] Polymer nanocomposites, which is a new class of polymeric materials based on the reinforcement of polymers using nanofillers, have attracted a great deal of interest in fields ranging from basic science to the industrial applications because it is possible to remarkably improve the physical properties of composite materials at lower filler loading.[1] Thus, the fabrication of polymer nanocomposites reinforced with various nanofillers is believed to a key technology on advanced composites for next generation.

Carbon nanotube (CNT) has attracted considerable attentions as novel nanoreinforcements in new kinds of polymer nanocomposites because of the combination of its unique extraordinary properties with high aspect ratio and small size.[6] In particular, excellent mechanical strength, thermal conductivity, and electrical properties of CNT have created a high level of activity in materials research and development for potential applications such as fuel cell, hydrogen storage, field emission display, chemical or biological sensor, and advanced polymer nanocomposites.[7–14] This feature has motivated a number of attempts to fabricate CNT/polymer nanocomposites in the development of high-performance composite materials.[15–22] In this regard, much research and development have been performed to date for achieving the practical realization of excellent properties of CNT for advanced polymer nanocomposites in a broad range of industrial applications. However, because of high cost and limited availability, only a few practical applications in industrial fields such as electronic and electric appliances have been realized to date.

Correspondence to: J. Y. Kim (junykim74@hanmail.net).

Poly(butylene terephthalate) (PBT) is a semicrystalline polymer with good mechanical properties and excellent processability, and it has been widely used as structural materials in the automotive, electrical, and electronic industries.[23–25] Recently, there are continuing practical demands for realizing higher performance of PBT with various processing conditions and thus making it possible to be utilized in various advanced industries. For these reasons, much research has been performed to date to extend and develop commercial applications of PBT as high-performance polymer nanocomposites using various nanoreinforcing fillers as well as to displace PBT.[26–28] Although promising, however, insufficient mechanical properties and thermal stability of the PBT composites have often hindered its potential application in a broad range of industrial fields.

From both an economic and industrial perspective, the major challenges for high-performance polymer nanocomposites are to fabricate polymer nanocomposites with low costs and to facilitate large scale-up for commercial applications. Currently, four processing techniques are in common use to incorporate CNT into the polymer matrix for fabricating CNT/polymer nanocomposites[15–20,29–34]: direct mixing, solution method, *in situ* polymerization, and melt blending. Of these processing techniques, a melt blending has been accepted as the simplest and the most effective method, particularly from a commercial perspective, because this process makes it possible to fabricate high-performance polymer nanocomposites at low process cost and facilitates commercial scale-up.[15–20,35–40] Furthermore, the combination of a small quantity of expensive CNT with conventional cheap thermoplastic polymers provides attractive possibilities for enhancing the physical properties of polymer nanocomposites using a cost-effective method.

In this study, the PBT nanocomposites reinforced with a small quantity of CNT were prepared by simple melt blending using a twin-screw extruder to create high-performance polymer nanocomposites with low process cost for practically possible application in a broad range of industry. The resultant nanocomposites were characterized by means of advanced rheometric expansion system (ARES) rheometer, dynamic mechanical thermal analysis (DMTA), transmission electron microscopy (TEM), scanning electron microscopy (SEM), differential scanning calorimetry (DSC), and thermogravimetric analysis (TGA) to clarify the effects of CNT on the physical properties of the PBT nanocomposites. We expect that this study will help in the preliminary understanding of the fabrication and enhanced properties of the PBT nanocomposites reinforced with a small quantity of CNT. In addition, our study suggests a simple and cost-effective method that will facilitate the industrial realization of CNT-filled PBT nanocomposites with enhanced physical properties.

EXPERIMENTAL

Materials

PBT was used as the thermoplastic polymer with an intrinsic viscosity of 1.1 dL/g and a melt-flow index of 20 g/min, supplied by Samyang Corp., Korea. The nanotubes used were multiwalled CNT (degree of purity $> 95\%$) synthesized by a thermal chemical vapor deposition process, purchased from Iljin Nanotech, Korea. According to the supplier, their length and diameter were 10–30 nm and 10–50 μm, respectively, indicating that their aspect ratio reaches 1000.

Preparation of nanocomposites

All materials were dried at 120°C *in vacuo* for at least 24 h before use to minimize the effects of moisture. The PBT nanocomposites were prepared by a melt-blending process in a Haake Rheometer (Haake Technik GmbH, Germany) equipped with the intermeshing corotating type of a twin-screw. The temperatures of the heating zone, from the hopper to the die, were set to 250, 260, 265, and 255°C, and the screw speed was fixed at 45 rpm. Before melt blending, PBT and CNT were physically premixed before being fed in the hopper of a twin-screw extruder to achieve better dispersion of CNT with the PBT matrix. For the fabrication of the PBT nanocomposites, PBT was melt-blended with the addition of CNT content, specified as 0.5, 1.0, and 2.0 wt % in the polymer matrix. Upon completion of melt blending, the extruded strands were cooled in the water bath and then cut into pellets using a rate-controlled pelletizer.

Characterizations

DMTA of the PBT nanocomposites was performed with a TA Instrument Q-800 DMTA using a tensile mode at a fixed frequency of 1 Hz, over the temperature range of 30–200°C at a heating rate of 5°C/min. The rheological properties of the PBT nanocomposites were performed on an ARES rheometer (Rheometric Scientific) in oscillation mode with the parallel-plate geometry using the plate diameter of 25 mm and the plate gap setting of $\sim$ 1 mm at 265°C, by applying a time-dependent strain, $\gamma(t) = \gamma_0 \sin(\omega t)$ and measuring resultant shear stress, $\gamma(t) = \gamma_0[G'\sin(\omega t) + G''\cos(\omega t)]$, where G' and G'' are storage and loss moduli, respectively. The frequency ranges varied between 0.05 and 450 rad/s, and the strain amplitude was applied to be within the linear

viscoelastic ranges. The morphology of the PBT nanocomposites was observed using a JEOL 2000-FX TEM imaging microtomed ultrathin slices of the PBT nanocomposite films with an accelerating voltage of 120 kV. SEM experiments were conducted using a JEOL JSM-6340F SEM with an accelerating voltage of 15 kV. The samples used for SEM observation were gold-coated *in vacuo* using ion sputtering before scanning to prevent charging in the electron beam. The mechanical properties of the PBT nanocomposites were measured at room temperature using an UTM 10E (United Calibration) according to the procedures in the ASTM D 638 and D 790 standards, respectively. The testing samples were prepared at 265°C with a Minimax laboratory molder CS-183 IM (CSI). At least five measurements were performed for each sample, and the results were averaged to obtain a mean value. The heat distortion temperature (HDT) of the PBT nanocomposites was measured under load (1.8 MPa) according to the procedures in the ASTM D 648 standard, and the HDT values represented the averages over at least five measurements. Thermal behavior of the PBT nanocomposites was measured with a TA Instrument 2010 DSC over the temperature range of 30–280°C at a scanning rate of 10°C/min under N_2 atmosphere. Samples with a typical mass of 6.5 ± 0.5 mg were encapsulated in sealed aluminum pans. Samples were first heated to 280°C at a heating rate of 10°C/min, maintained at that temperature for 8 min to eliminate any previous thermal history, and then cooled to room temperature at a cooling rate of 10°C/min. The wide-angle X-ray diffraction (WAXD) analysis was performed with a Rigaku Denki X-ray diffractometer using Ni-filtered Cu Kα X-rays ($\lambda = 0.1542$ nm), and the diffracting intensities were recorded at steps of every $2\theta = 0.05°$ over the rage of $5° < 2\theta < 45°$. TGA of the PBT nanocomposites was performed with a TA Instrument SDF-2960 TGA over the temperature range of 30–800°C at a heating rate of 10°C/min under N_2 atmosphere.

RESULTS AND DISCUSSION

Rheological properties

The complex viscosity ($|\eta^*|$) of the PBT nanocomposites as a function of frequency is shown in Figure 1. The $|\eta^*|$ values of pure PBT and the PBT nanocomposites were decreased with increasing frequency, indicating a non-Newtonian behavior over the frequency range measured. The shear thinning behavior observed in the PBT nanocomposites was attributed to random orientation and entangled molecular chains in the polymer nanocomposites during the applied shear force. The effect of CNT on

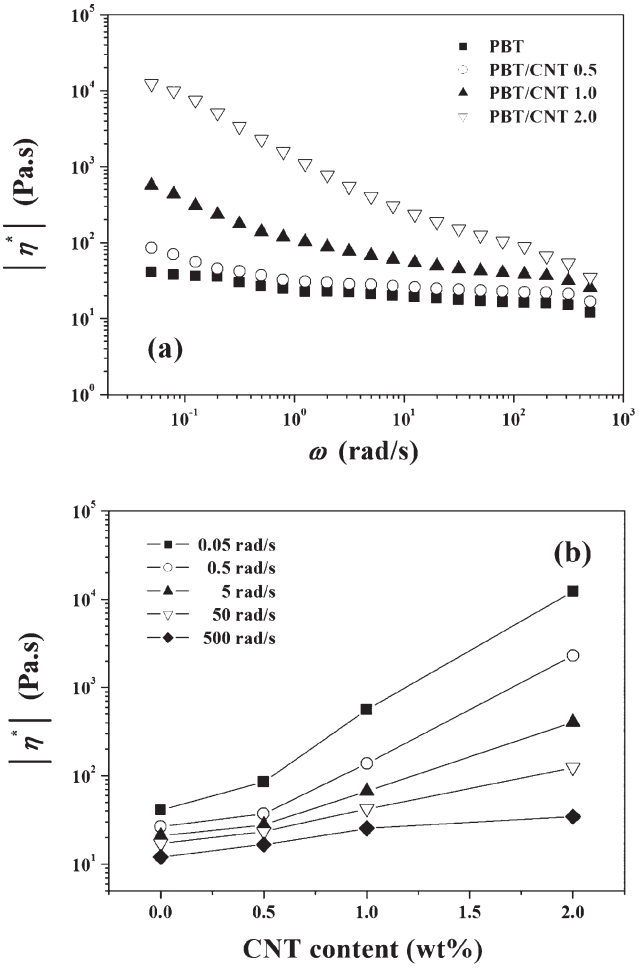

Figure 1 (a) Complex viscosity of the PBT nanocomposites as a function of frequency and (b) the variations of complex viscosity of the PBT nanocomposites with CNT content at different frequencies.

the complex viscosity of the PBT nanocomposites was more significant at low frequency than at high frequency, and this enhancing effect was decreased with increasing frequency because of the strong shear thinning behavior of the PBT nanocomposites induced by CNT. As shown in Figure 1(b), the PBT nanocomposites exhibited higher $|\eta^*|$, particularly at low frequency when compared with pure PBT, indicating the formation of interconnected or network-like structures as a result of particle–particle and particle–polymer interactions.[41] The PBT nanocomposites exhibited shear thinning behavior, resulting from the breakdown of these structures with increasing frequency. The increase in the $|\eta^*|$ of the PBT nanocomposites was closely related to the increase in the storage modulus, which will be elaborated in the following section.

To understand the effect of CNT on the rheological behavior of the PBT nanocomposites, it is very instructive to characterize the variations of the shear thing exponent for the PBT nanocomposites.[42] In the

TABLE I
Variations of Low-Frequency Slope of $|\eta^*|$, G', and G'' versus ω of the PBT Nanocomposites

Materials	Slope of $\|\eta^*\|$ versus ω	Slope of G' versus ω	Slope of G'' versus ω
PBT	−0.1389	0.7639	0.7342
PBT/CNT 0.5	−0.1548	0.4286	0.5081
PBT/CNT 1.0	−0.3643	0.4030	0.5043
PBT/CNT 2.0	−0.7592	0.3128	0.4255

case of an ideal Newtonian fluid, the shear thinning exponent approaches or equals 0, and the viscosity is independent of the frequency, thereby exhibiting terminal flow behavior, whereas for the polymer nanocomposites, as the shearing thinning behavior develops, the shearing thinning exponent increases with increasing filler concentration.[42–45] The shear thinning exponent of the PBT nanocomposites can be obtained from the slope of the plot of $|\eta^*|$ versus ω. As shown in Table I, the shear thinning exponent of the PBT nanocomposites slightly decreased with the introduction of CNT, and this effect was more pronounced at high CNT content, indicating the significant dependence of the shear thinning behavior of the PBT nanocomposite on CNT content.

The storage modulus (G') and loss modulus (G'') of the PBT nanocomposites as a function of frequency are shown in Figure 2. The values of G' and G'' for the PBT nanocomposites increased with increasing frequency, and this enhancing effect was more pronounced at low frequency. This rheological response is similar to the relaxation behavior of the typical filled-polymer composite systems.[42–45] If polymer chains are fully relaxed and exhibit a characteristic homopolymer-like terminal behavior, the flow curves of polymers can be expressed by a power law of $G' \propto \omega^2$ and $G'' \propto \omega$.[46] Krishnamoorti and Giannelis[45] reported that the slopes of G' and G'' for polymer/layered silicate nanocomposites were much smaller than 2 and 1, respectively, suggesting that large deviations in the presence of a small quantity of layered silicate were caused by the formation of a network-like structures in the molten state. The slopes of the terminal zone of G' and G'' for the PBT nanocomposites are shown in Table I. This result indicated the nonterminal behavior with the power-law dependence for G' and G'' of the PBT nanocomposites. Similar nonterminal low-frequency rheological behavior has been observed in the ordered block copolymers and the smectic liquid-crystalline small molecules.[47,48] The decrease in the slopes of G' and G'' for the PBT nanocomposites with increasing CNT content was explained by the fact that the nanotube–nanotube or the polymer–nanotube interactions can lead to the formation of the interconnected or network-like structures, resulting in the pseudo solid-like behavior of the PBT nanocomposites. As shown in Figure 2, the extent of the increase in G' of the PBT nanocomposites was higher than that of G'' over the frequency range measured, and the values of G' and G'' of the PBT nanocomposites were higher than those of pure PBT, particularly at low frequency. This result demonstrated that the interconnected or network-like structures were formed in the PBT nanocomposites via nanotube–nanotube or polymer–nanotube interactions in the presence of CNT, resulting in more elasticity of the PBT nanocomposites than pure PBT. As the applied frequency increased, the interconnected or network-like structures were broken down because of the high levels of shear force, and the PBT nanocomposites exhibited almost similar or slight higher G' and G'' values than those of pure PBT at high frequency.

The variations of tan δ as a function of frequency for the PBT nanocomposites are shown in Figure 3. Shear deformation can lead to partial orientation of the molecules in polymer chains, and tan δ

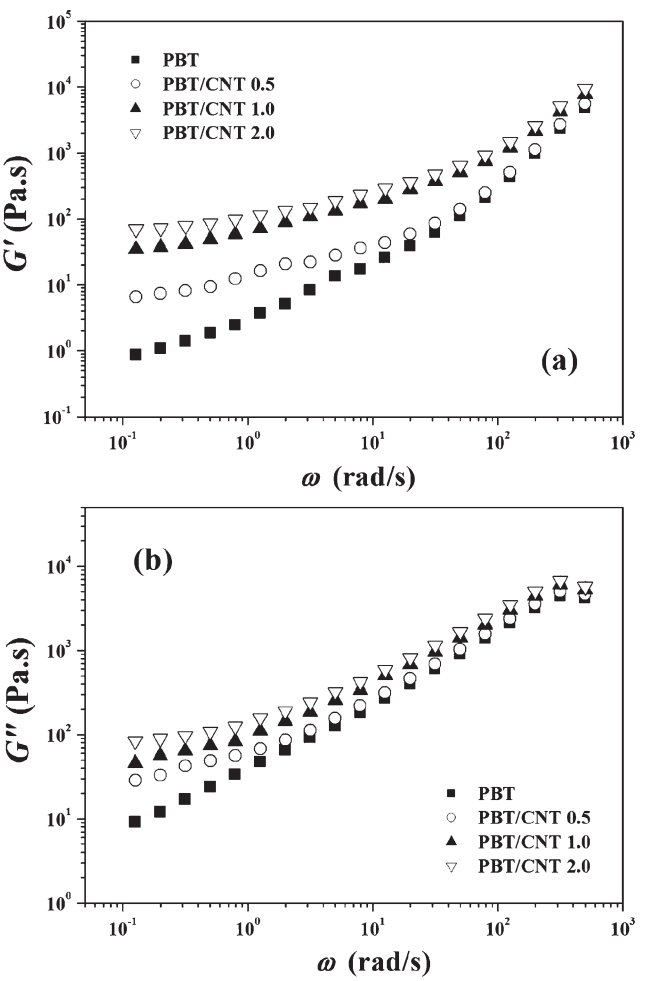

Figure 2 (a) Storage modulus (G') and loss modulus (G'') of the PBT nanocomposites as a function of frequency.

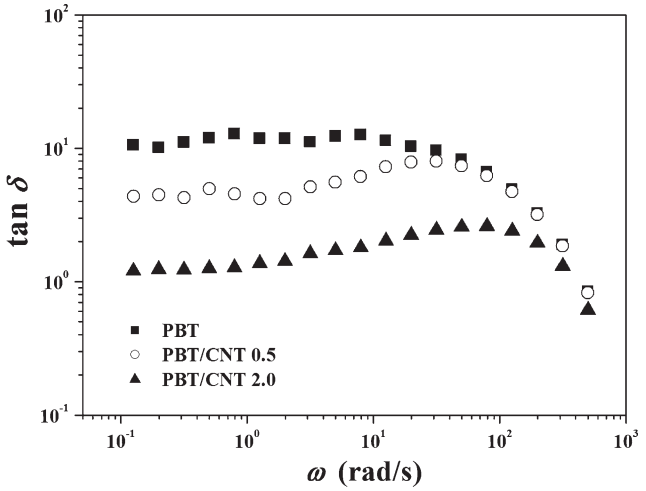

Figure 3 Variations of the tan δ as a function of frequency for the PBT nanocomposites.

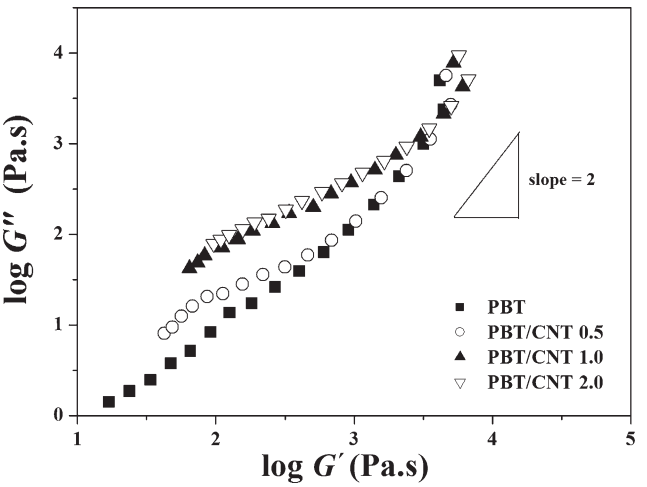

Figure 5 Plots of log G' versus log G'' for the PBT nanocomposites.

decreased with increasing frequency. The maximum of tan δ of the PBT nanocomposites shifted toward high-frequency region with increasing CNT content, indicating the formation of densely interconnected or network-like structures in the PBT nanocomposites.[16] The plots of the phase angle (δ) versus the absolute values of the complex modulus ($|G^*|$) for the PBT nanocomposites, which is known as the Van Gulp-Palmen plot,[49] are shown in Figure 4. It can be seen that a significant change in the δ values occurred with the introduction of CNT. For the PBT nanocomposites, the phase angle decreased with decreasing the complex modulus, indicating that the incorporation of CNT into the PBT matrix enhanced the elastic behavior of the PBT nanocomposites. The plots of log G' versus log G'' for the PBT nanocomposites are shown in Figure 5. In general, this plot provides a master curve with a slope of 2 for isotropic and homogeneous polymer melts, irrespective of temperature.[50] However, the PBT nanocomposites did not provide a perfect single master curve and exhibited the shifting and the change of the slope of the plot with the introduction of CNT. The slopes in the terminal regime of the PBT nanocomposites were less than 2, indicating that the PBT nanocomposite systems were heterogeneous and they underwent some chain conformational changes because of the interconnected or network-like structures via the nanotube–nanotube or nanotube–polymer interactions in the presence of CNT.[41] However, over the higher G'' values, the slopes of the PBT nanocomposites increased and approached similar slope of pure PBT, indicating that the interconnected or network-like structures formed in the nanocomposites in the presence of CNT were broken down by high levels of shear force.

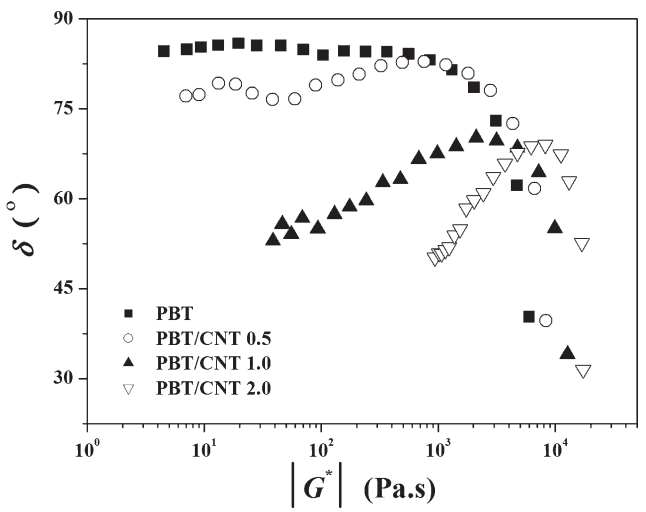

Figure 4 Plots of the phase angle (δ) versus the complex modulus ($|G^*|$) of the PBT nanocomposites.

Dynamic mechanical properties

The dynamic mechanical properties of the PBT nanocomposites are shown in Figure 6. There is a significant dependence of the storage modulus (E') and the tan δ for the PBT nanocomposites on the temperature and the presence of CNT. As the molecular motions within the polymer nanocomposites change, the storage modulus of the polymer nanocomposites varied with the temperature. The E' values of the PBT nanocomposites decreased rapidly, whereas the tan δ underwent a maximum when the polymer nanocomposites were heated through the glass transition region. The incorporation of CNT into the PBT matrix significantly increased the E' values of the PBT nanocomposites, which may be attributed to the physical interactions between PBT matrix and CNT with high aspect ratio and large

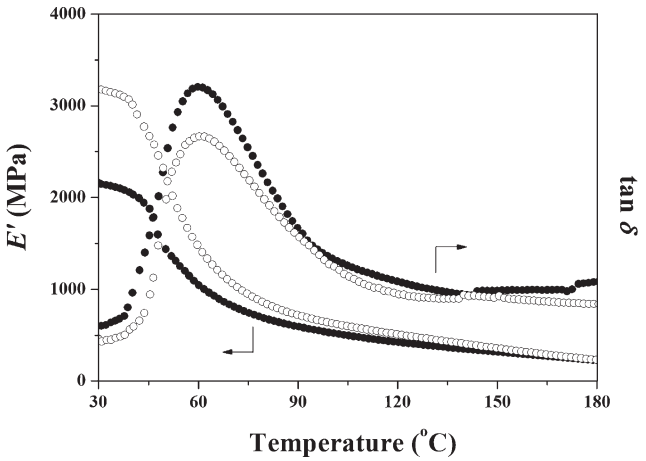

Figure 6 Dynamic mechanical properties of the PBT nanocomposites as a function of temperature (solid circles represent pure PBT and the open circles represent the PBT/CNT 2.0 nanocomposites).

surface areas as well as the stiffening effect of CNT as nanoreinforcing fillers, making it possible for them to allow efficient load transfer in the PBT nanocomposites. As shown in Figure 6, the tan δ peak of the PBT nanocomposites as a function of temperature was not significantly affected in the presence of CNT, whereas the peak height was decreased with the introduction of CNT.

Morphology

The SEM microphotographs of CNT and the PBT nanocomposites are shown in Figure 7. CNT exhibited highly curved and randomly coiled features and typically tends to bundle together or some agglomerated organization because of the intrinsic van der Waals attractions between the individual nanotubes in combination with high aspect ratio and large surface area.[51] As shown in Figure 7(b), CNTs were randomly oriented and formed the interconnected or network-like structures in the PBT nanocomposites. CNT with a small size, high aspect ratio, and large surface area are often subjected to self-agglomeration or bundle formation at higher concentration of CNT and thus easily form interconnected or network-like structures in the molten polymer matrix.[52] Some CNT bundles were pulled out from the PBT matrix and some of the nanotube bundles were individually dispersed in the polymer matrix. As shown in Figure 8, the TEM image of the PBT nanocomposites containing 0.5 wt % of CNT showed that the dispersion of the CNT was quite good. However, at high CNT content, less uniformly dispersed and highly entangled CNT structures could be observed in the PBT nanocomposites. On a large scale, CNTs were uniformly dispersed in the PBT matrix despite some agglomerated CNT structures, and the PBT nanocomposites exhibited relatively more uniform dispersion of CNT in the PBT matrix particularly at lower CNT content in comparison with the nanocomposites at higher CNT content.

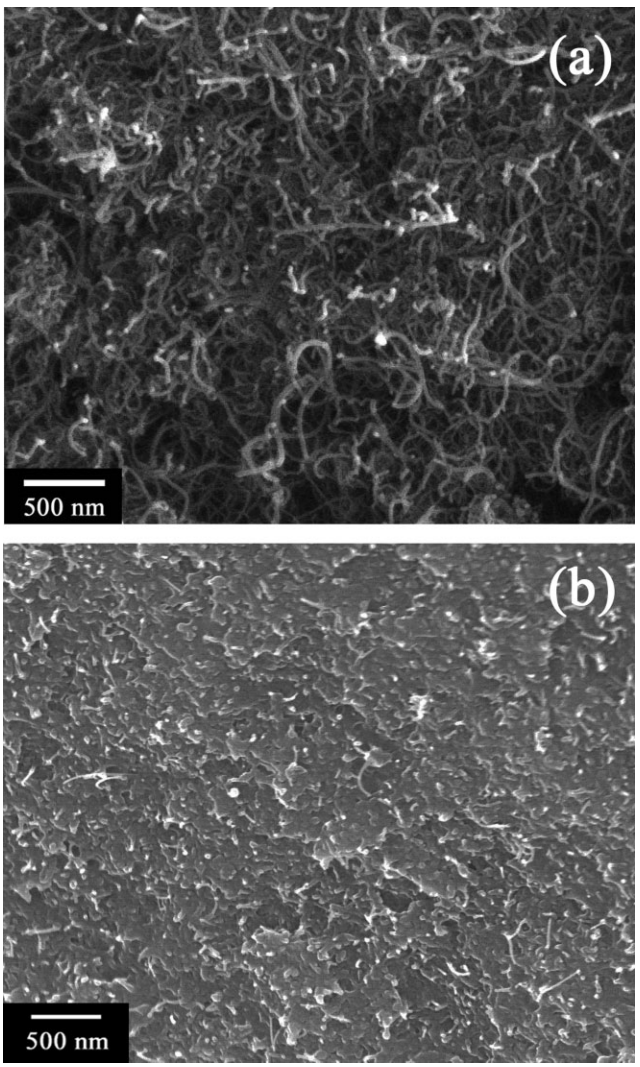

Figure 7 SEM images of (a) CNT and (b) the PBT nanocomposites containing 2.0 wt % of CNT.

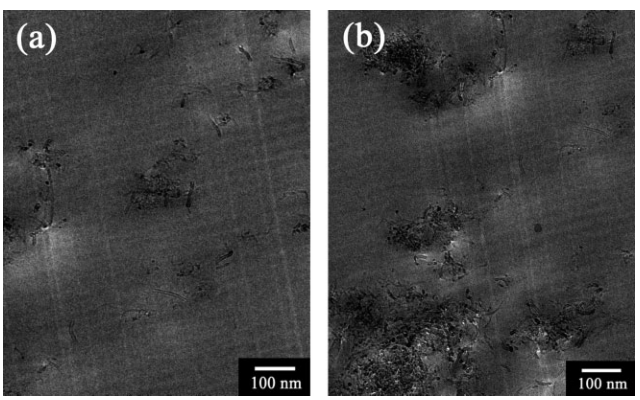

Figure 8 TEM images of the PBT nanocomposites containing (a) 0.5 and (b) 2.0 wt % of CNT.

Mechanical properties

The variations of mechanical properties of the PBT nanocomposites with CNT content are shown in Figure 9. There was a significant dependence of the mechanical properties of the PBT nanocomposites on CNT content. The incorporation of a small quantity of CNT into the PBT matrix can substantially improve the mechanical properties of the PBT nanocomposites because of the nanoreinforcing effect of CNT with high aspect ratio and their uniform dispersion in the PBT matrix. In comparison with pure PBT, the PBT nanocomposites exhibited higher tensile strength and tensile modulus. For instance, on the incorporation of the CNT, the tensile strength and tensile modulus were significantly increased by 35.1 and 21.7%, respectively. This enhancing effect of CNT on the tensile strength and tensile modulus of the PBT nanocomposites was more significant at low CNT content when compared with high CNT content. The fact that the improvement in the mechanical properties of the PBT nanocomposites was not increased at higher CNT content as expected, in comparison with that at low CNT content, was explained by the characteristics of CNT that tended to bundle together because of their intrinsic van der Waals attractions between the individual nanotubes in combination with high aspect ratio and large surface area and could lead to some agglomeration, causing the stress concentration phenomenon and preventing efficient load transfer to the polymer matrix.[1–3] Similar observation has been reported by Gorga and Cohen[53] that for CNT/polypropylene (PP) nanocomposite systems, adding a low level of CNT into the PP matrix improved the mechanical properties of CNT/PP nanocomposites, while at high CNT content, their mechanical properties decreased via stress concentration by the nanotube aggregation, and they suggested that poor adhesion between CNT and polymer matrix as well as imperfection and defects in the nanotube structures resulted in the reduced mechanical properties of polymer nanocomposites. For achieving further enhanced mechanical properties of the PBT nanocomposites, the improvement in the dispersion rate of CNT and the interfacial adhesion between two phases should be required; our current research is also aimed at that topic through chemical modification of CNT with various functional groups. The elongation at break of the PBT nanocomposites decreased with the introduction of CNT, indicating that the PBT nanocomposites became somewhat brittle when compared with pure PBT because of the increased stiffness of the PBT nanocomposites and the microvoid formed around the nanotubes during the tensile testing. As shown in Figure 9(b), the flexural strength and flexural modulus of the PBT nanocomposites increased with the introduction of CNT. This enhancement of the flexural strength/modulus was attributed to the reinforcement of the PBT matrix by incorporating the dispersed CNT and the moderate transfer of the applied stress between PBT matrix and CNT. In addition, the enhancement of the flexural modulus of the PBT nanocomposites was related to the variations of the HDT values, which will be elaborated in the following section.

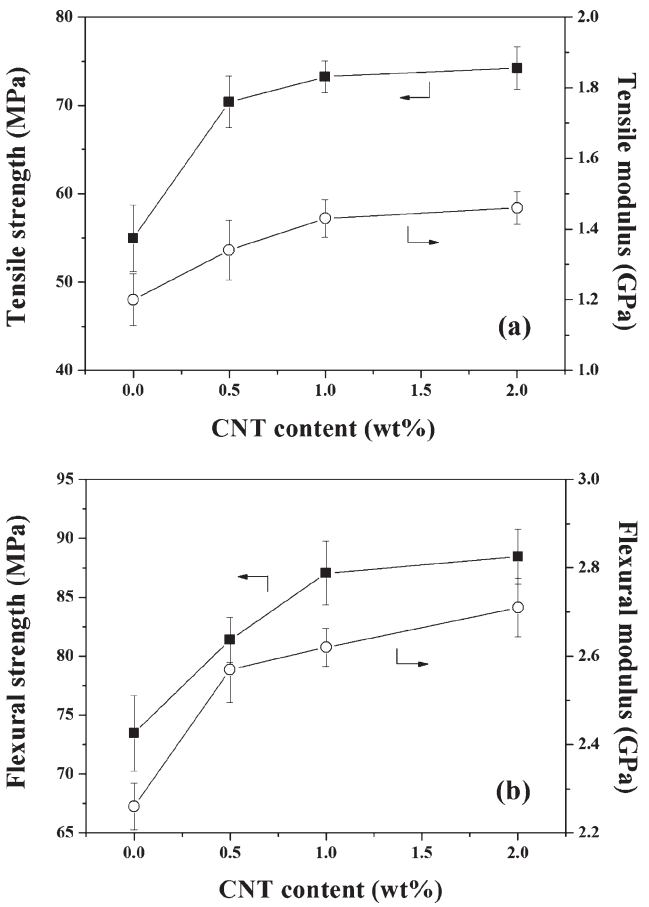

Figure 9 Variations of (a) the tensile strength and tensile modulus and (b) the flexural strength and flexural modulus of the PBT nanocomposites with CNT content.

For characterizing the effect of CNT content on the mechanical properties of the PBT nanocomposites, it is also instructive to compare the reinforcing efficiency of CNT for a given concentration in the PBT nanocomposites. The variations of the reinforcing efficiency of CNT in the PBT nanocomposites are shown in Figure 10. In this study, the reinforcing efficiency of CNT is defined as the normalized mechanical properties of the PBT nanocomposites with respect to those of pure PBT. The enhancing effect of the mechanical properties by incorporating CNT was more significant at low CNT content than at high content, indicating that a low CNT loading was more effective in improving the overall mechanical properties of the PBT nanocomposites. At higher

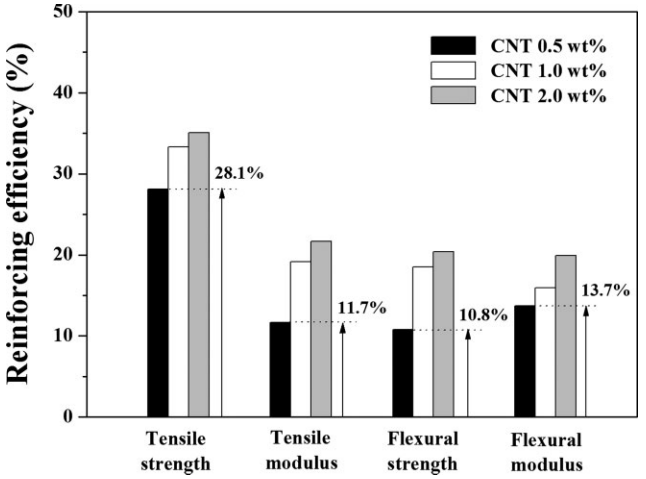

Figure 10 Variations of the reinforcing efficiency of CNT on the mechanical properties of the PBT nanocomposites [reinforcing efficiency (%) = $(M_c - M_m)/M_m \times 100$, where M_c and M_m represent the mechanical properties, including tensile strength, tensile modulus, flexural strength, and flexural modulus, of the PBT nanocomposites and pure PBT, respectively].

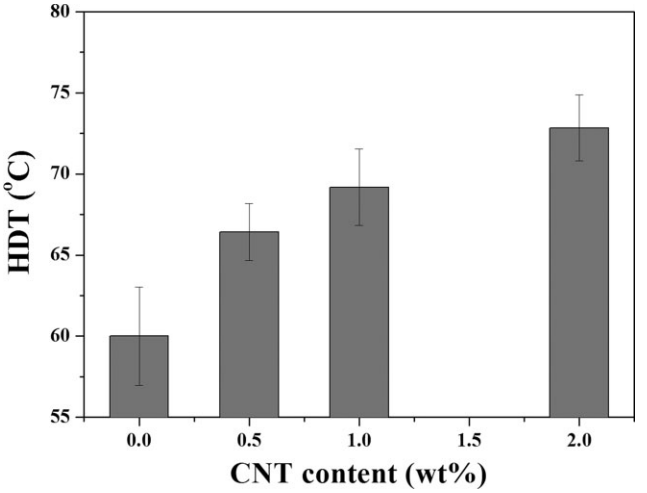

Figure 11 Variations of the heat distortion temperatures (HDT) of the PBT nanocomposites.

CNT content, CNT tends to bundle together and to form some agglomeration because of intrinsic van der Waals attractions between the individual nanotubes and lead to the stress concentration phenomenon, thus preventing efficient load transfer to the polymer matrix. This result demonstrates that the incorporation of relatively small quantity of CNT into the PBT matrix is more effective in the enhancement of the overall mechanical properties of the PBT nanocomposites induced by high nanoreinforcing efficiency of CNT as well as good dispersion of CNT in the PBT matrix at lower concentration.

Heat distortion temperature

The elevated temperature property, typically estimated by the HDT, plays a critical role in determining the performance of engineering plastics. The HDT represents the upper limit of the dimensional stability of polymers in service without significant physical deformations under a normal load and thermal effect, providing important information for product design.[54,55] The HDT can be influenced by various factors such as the melt and mold temperatures, the nucleating agent, and various processing conditions, which is often related to the mechanical behavior of polymer composites. The variations of the HDT values for the PBT nanocomposites with CNT content are shown in Figure 11. The HDT values of the PBT nanocomposites increased with increasing CNT content, which may be explained by the improvement in the modulus of the PBT nanocomposites. According to Nielsen's prediction,[56] the variation of the HDT value was related to the behavior of flexural modulus with the filler content. The increase in the HDT values of the PBT composites with increasing CNT content was in good agreement with the results of the flexural modulus of the PBT nanocomposites as shown in Figure 9(b), conforming to the Nielsen's prediction. The increased HDT values of the PBT composites were attributed to the improvement of the flexural modulus with increasing CNT content. In the HDT measurements, the ability of a polymeric material to retain stiffness with increasing temperature is important for a high HDT value.[57] As shown in Figure 6, the introduction of CNT could make it possible for the PBT nanocomposites to maintain moderate modulus and high temperature stiffness with increasing temperature, which was also contributed to the enhancement of the HDT values of the PBT nanocomposites. Thus, the improvement in the HDT values of the PBT composites resulted from the enhanced flexural modulus of the PBT nanocomposites as well as the increased ability of the PBT nanocomposites to retain high stiffness induced by CNT.

TABLE II
DSC Results of the PBT Nanocomposites with CNT Content

Materials	T_g[a] (°C)	T_m[a] (°C)	ΔH_m[a] (J/g)	T_c[b] (°C)	ΔT[c] (°C)
PBT	56.9	224.4	41.7	176.8	47.6
PBT/CNT 0.5	56.2	224.6	42.4	190.3	34.3
PBT/CNT 1.0	56.7	223.9	43.1	191.4	32.5
PBT/CNT 2.0	57.1	224.3	44.3	192.2	32.1

[a] Values obtained from the DSC heating traces at a heating rate of 10°C/min.
[b] Values obtained from the DSC cooling traces at a cooling rate of 10°C/min.
[c] Degree of supercooling, $\Delta T = T_m - T_c$.

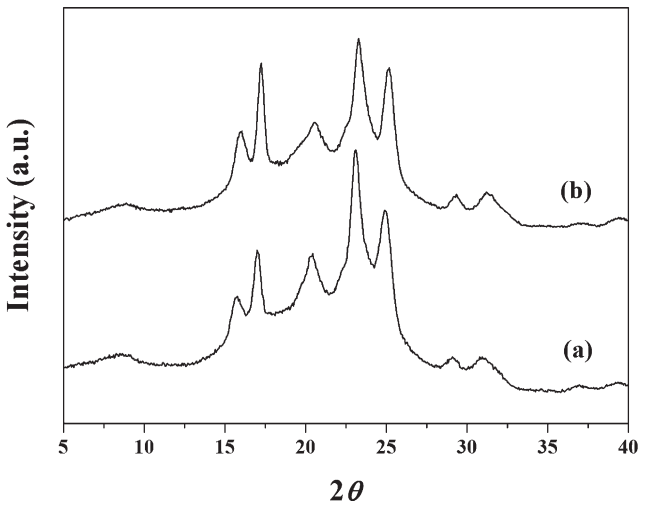

Figure 12 Wide-angle X-ray diffraction patterns of (a) pure PBT and (b) the PBT/CNT 2.0 nanocomposites.

Thermal behavior

The DSC thermograms of the PBT nanocomposites are shown in Table II. The incorporation of CNT into the PBT matrix has less effect on the values of T_g and T_m of the PBT nanocomposites. The T_c values were significantly increased with the introduction of CNT, and this effect was more pronounced at low CNT content. This result indicates the efficiency of CNT as strong nucleating agents for the crystallization of PBT, suggesting the enhancement of the crystallization of the PBT nanocomposites in the presence of CNT. As shown in Table II, the increase in the crystallization temperature of the PBT nanocomposites with increasing CNT content, together with the fact that the degree of supercooling (ΔT) for crystallization decreased with increasing CNT content, suggested that the CNT could act as effective nucleating agents in the PBT matrix, resulting in the enhancement of the PBT crystallization. Thus, the incorporation of a small quantity of CNT into the PBT matrix can effectively enhance the crystallization of the PBT nanocomposites through heterogeneous nucleation. Similar observations have been reported for CNT-filled polymer nanocomposites, i.e., the accelerated crystallization by the introduction of CNT through heterogeneous nucleation.[15–19]

WAXD analysis was conducted on the PBT nanocomposites to investigate the effect of the CNT on the structure of the PBT nanocomposites. WAXD patterns of the PBT nanocomposites are shown in Figure 12. For pure PBT, strong diffraction peaks observed at near 15.8°, 17.1°, 20.4°, 23.1°, and 25.0°, respectively, were assigned to the (0-11), (010), (011), (100), and (1-11) reflections, indicating the α-form of the PBT crystals with a triclinic configuration.[58] The characteristics peaks of pure PBT were also observed for the PBT nanocomposites, and the position of their peaks remained almost unchanged with the introduction of the CNT, despite some changes in the peak intensity. This result demonstrates that the incorporation of CNT into the PBT matrix does not change the crystal structure of the PBT nanocomposites. The crystallinity of the PBT nanocomposites was slightly increased with the introduction of CNT, which may be explained by the supercooling temperature. In the PBT nanocomposites, CNT acts as a strong nucleating agent in the PBT matrix, and the crystallization temperature shifts to higher temperature, implying that the supercooling of the PBT nanocomposites was decreased with the introduction of CNT (Table II). When polymers crystallized with less supercooling, it crystallized more perfectly than with more supercooling,[59] and thus, the crystallinity of the PBT nanocomposites slightly increased with the introduction of CNT.

Thermal stability and thermal decomposition kinetics

Thermal stability of polymer nanocomposites plays a critical role in determining the limit of working temperature and the environmental conditions for use of polymer nanocomposites, which is closely related to their thermal decomposition temperatures and decomposition rates.[60] The TGA thermograms of the PBT nanocomposites with CNT content are shown in Figure 13(a), and their results are summarized in Table III. TGA curve of the thermal decomposition for pure PBT exhibited only one dominant decline of the residual weight, indicating the random scission of the PBT main chain as the prevailing decomposition reaction.[61] The patterns of TGA curves for the PBT nanocomposites were similar to that of PBT, indicating that the thermal decomposition of the PBT nanocomposites may primarily stem from PBT. The incorporation of CNT into the PBT matrix can increase the thermal decomposition temperatures and the residual yields of the PBT nanocomposites, indicating that the presence of CNT can lead to the stabilization of the PBT matrix, resulting in the enhanced thermal stability of the PBT nanocomposites. CNT can effectively act as physical barriers to hinder the transport of volatile decomposed products out of the PBT nanocomposites during thermal decomposition. Similar observation has been reported that CNT layers exhibited a good barrier effect on the thermal degradation process, leading to the retardation of the weight-loss rate of thermal degradation products as well as the thermal insulation of polymers in the nanocomposites.[62]

The TGA kinetic analysis was conducted on the PBT nanocomposites to clarify the effects of CNT on the thermal stability of the PBT nanocomposites. The

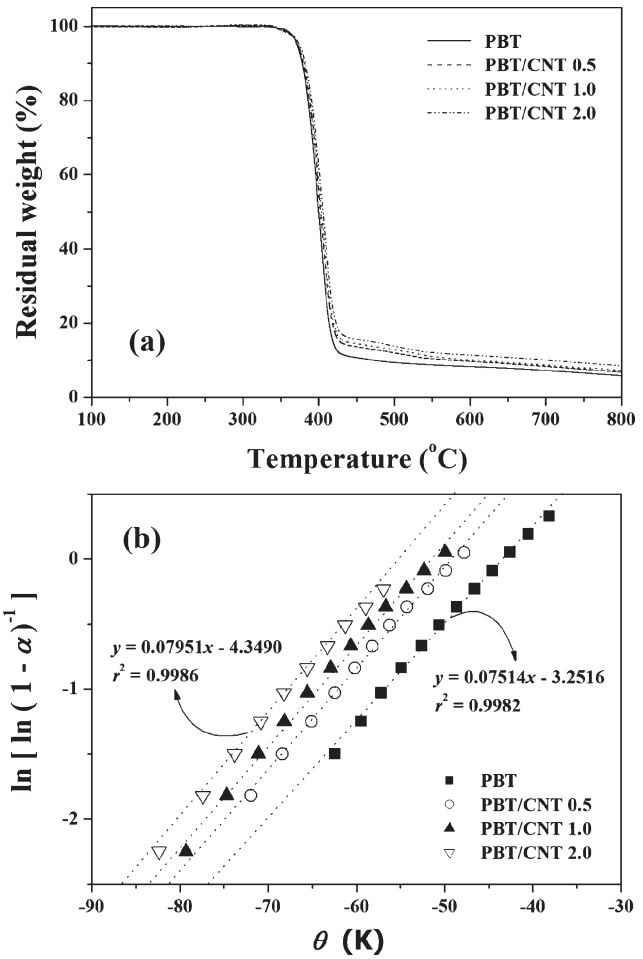

Figure 13 (a) TGA thermograms of the PBT nanocomposites and (b) the plots of $\ln[\ln(1-\alpha)^{-1}]$ versus θ as shown for the PBT nanocomposites.

thermal decomposition temperatures and decomposition kinetic parameters, including the thermal decomposition temperatures at 5 and 10% of the weight loss (T_{d5} and T_{d10}), the temperature at maximum rate of the weight loss (T_{dm}), the integral procedure decomposition temperature (IPDT), and the activation energy for decomposition (E_a) are in common use to characterize the thermal stability of polymer nanocomposites.[63] As shown in Table III, the thermal stability factors, including T_{d5}, T_{d10}, T_{dm}, and IPDT, of the PBT nanocomposites were higher than that of pure PBT and they tended to increase with CNT content. This result indicated that the incorporation of a small quantity of CNT into the PBT matrix could substantially improve the thermal stability of the PBT nanocomposites, and the thermal volatilization of pure PBT could be retarded in the presence of CNT during thermal decomposition. Because the PBT molecular chains were more difficult to thermally decompose with the introduction of CNT, the residual yields of the PBT nanocomposites also slightly increased with the CNT content. In the PBT nanocomposites, the introduced CNT to induce protective barriers against thermal decomposition for organic species retarded the thermal decomposition of the PBT nanocomposites, which was attributed to the physical barrier effects induced by CNT acting as the mass and heat transfer barriers.[64] As a consequence, the thermal stability of the PBT nanocomposites can be enhanced with the introduction of a small quantity of CNT. Kashiwagi et al.[62] reported that CNT layers exhibited a good barrier effect on the thermal degradation process and could lead to the retardation of the weight-loss rate of thermal degradation products as well as the slow down of thermal decomposition with the introduction of CNT, insulation of polymers in the polymer nanocomposites, resulting in the enhanced thermal stability of CNT/polymer nancoomposites. TGA results demonstrate that a small quantity of CNT is beneficial to act as the thermal decomposition-resistant nanoreinforcing fillers in the PBT nanocomposites.

The activation energy for the thermal decomposition (E_a) of the PBT nanocomposites can be estimated from the TGA thermograms by the Horowitz-Metzger integral kinetic method[65] as follows:

$$\ln\left[\ln(1-\alpha)^{-1}\right] = \frac{E_a\theta}{RT_{dm}^2} \quad (1)$$

where α is the weight loss; θ is the variable auxiliary temperature defined as $\theta = T - T_{dm}$, and R is the universal gas constant. The E_a values of the PBT nanocomposites can be estimated from the slope of

TABLE III
Effect of CNT on the Thermal Stability of the PBT Nanocomposites

Materials	T_5[a] (°C)	T_{10}[a] (°C)	T_{dm}[b] (°C)	A	K	IPDT[c] (°C)	W_R[d] (%)
PBT	371.3	378.2	400.9	0.5222	1.1253	481.0	5.82
PBT/CNT 0.5	372.9	380.2	402.8	0.5336	1.1465	499.8	6.81
PBT/CNT 1.0	373.9	381.1	404.4	0.5372	1.1575	507.5	7.32
PBT/CNT 2.0	374.8	382.7	407.5	0.5448	1.1847	529.9	8.51

[a] The decomposition temperatures at the weight-loss of 5 and 10%, respectively.
[b] The decomposition temperature at the maximum rate of the weight loss.
[c] The integral procedure decomposition temperature, $IPDT = AK(T_1 - T_1) + T_1$ (where A is the area ratio of total experimental curve divided by total TGA thermograms; K is the coefficient of A; T_1 is the initial experimental).

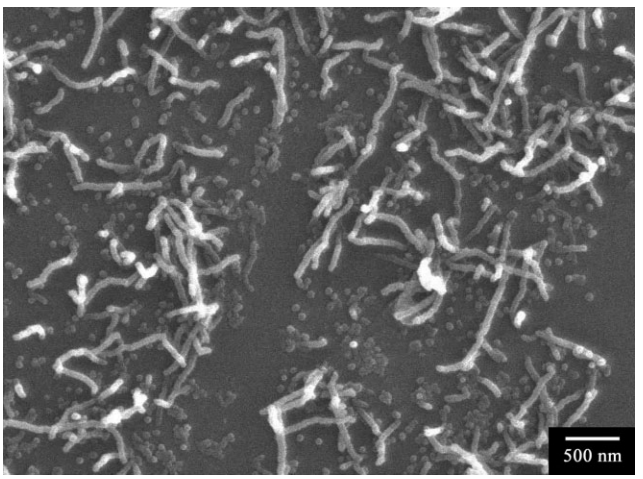

Figure 14 SEM image of the residues of the PBT nanocomposites containing 2.0 wt % of CNT after thermal decomposition process.

the plot of $\ln[\ln(1-\alpha)^{-1}]$ versus as shown in Figure 13(b). The E_a values of the PBT nanocomposites were 295.0, 297.5, and 306.2 kJ/mol, respectively. Compared with pure PBT (E_a = 283.8 kJ/mol), the higher E_a values of the PBT nanocomposites were more thermally stable than pure PBT. This result indicated that the presence of CNT in the nanocomposites increased the activation energy for thermal decomposition of the PBT matrix. The introduction of CNT, effectively acting as physical barriers or protective layers against the thermal decomposition, could lead to the enhanced thermal stability of CNT-filled polymer nanocomposites. For the PBT nanocomposites, the Horowitz-Metzger analysis demonstrates that the incorporation of CNT into the PBT matrix could increase the E_a values of the PBT nanocomposites, which was related to the enhancement of the thermal stability of the PBT nanocomposites. In addition, it can be deduced that the E_a values of the PBT nanocomposites exhibited a good reliance on describing the thermal decomposition kinetics of the PBT nanocomposites, which was confirmed by the fact that the values of the correlation coefficient (r^2) were greater than 0.99.

The morphology of the residues of the PBT/CNT 2.0 nanocomposites after thermal decomposition is shown in Figure 14. The PBT nanocomposites exhibited the dispersed structure of CNT in the PBT matrix kept after thermal decomposition, despite some collapse or loss of their form. This feature may also contribute to the enhancement of the thermal stability of the PBT nanocomposites. This enhancing effect of CNT resulted from high thermal resistance of CNT to increase the energy required for thermal decomposition as well as physical barrier effect against thermal decomposition.[64]

CONCLUSIONS

Polyester nanocomposites based on PBT and a small quantity of CNT for improving the physical properties of polymer nanocomposites were prepared by simple melt blending in a twin-screw extruder. There is significant dependence of the rheological, thermal, and mechanical properties of the PBT nanocomposites on CNT content. The nonterminal behavior of the PBT nanocomposites was caused by nanotube–nanotube or polymer–nanotube interactions, and the dominant nanotube–nanotube interactions at high CNT content resulted in the formation of the interconnected or network-like structures of CNT. The presence of a small quantity of CNT can effectively act as good nucleating agent in the PBT nanocomposites, resulting in the enhancement of the PBT crystallization through heterogeneous nucleation. The mechanical properties of the PBT nanocomposites were significantly improved with the introduction of CNT, and this enhancing effect was more pronounced at lower CNT content, resulting from the nanoreinforcing effect of CNT with high aspect ratio and large surface areas to allow the efficient load transfer from the polymer matrix to the nanotube. The HDT of the PBT composites increased with CNT content, which was related to the enhanced flexural modulus of the PBT nanocomposites as well as the increased capability of the PBT nanocomposites to retain high stiffness induced by CNT. The Horowitz-Metzger analysis demonstrated that the incorporation of CNT into the PBT matrix could increase the activation energy for thermal decomposition and lead to the enhancement of the thermal stability of the PBT nanocomposites, resulting from physical barrier effects of CNT against thermal decomposition.

References

1. Paul, D. R.; Robeson, L. M. Polymer 2008, 49, 3187.
2. Bokobza, L. Polymer 2007, 48, 5279.
3. Ajayan, P. M. Chem Rev 1999, 99, 1787.
4. Kim, J. Y.; Kim, S. H.; Kang, S. W.; Chang, J. H. Macromol Res 2006, 14, 146.
5. Kim, J. Y.; Kim, D. K.; Kim, S. H. Polym Compos 2009, in press.
6. Ebbesen, T. W. Annu Rev Mater Sci 1994, 24, 235.
7. Liu, C.; Fan, Y. Y.; Liu, M.; Cong, H. T.; Dresselhaus, M. S. Science 1999, 286, 1127.
8. Ishihara, T.; Kawahara, A.; Nishiguchi, H.; Yoshio, M.; Takita, Y. J Power Sources 2001, 97, 129.
9. Wu, M.; Shaw, L. Int J Hydrogen Energy 2005, 30, 373.
10. De Heer, W. A.; Chatelain, A.; Ugarte, D. Science 1995, 270, 1179.
11. Fan, S.; Chapline, M. G.; Franklin, N. R.; Tombler, T. W.; Casell, A. M.; Dai, H. Science 1999, 283, 512.
12. Kim, P.; Lieber, C. M. Science 1999, 286, 2148.
13. Kong, J.; Franklin, N.; Zhou, C.; Peng, S.; Cho, J. J.; Dai, H. Science 2000, 287, 622.

14. Alan, B.; Dalton, A. B.; Collins, S.; Muñoz, E.; Razal, J. M.; Ebron, V. H.; Ferraris, J. P.; Coleman, J. N.; Kim, B. G.; Baughman, R. H. Nature 2003, 423, 703.
15. Kim, J. Y.; Kim, S. H. In Polymer Nanocomposite Research Advances; Thomas, S.; Zaikov, G. E., Eds.; Nova Science Publishers: New York, 2008; Chapter 7.
16. Kim, J. Y.; Han, S. I.; Hong, S. Polymer 2008, 49, 3335.
17. Kim, J. Y.; Han, S. I.; Kim, S. H. Polym Eng Sci 2007, 47, 1715.
18. Kim, J. Y.; Park, H. S.; Kim, S. H. J Appl Polym Sci 2007, 103, 1450.
19. Kim, J. Y.; Park, H. S.; Kim, S. H. Polymer 2006, 47, 1379.
20. Kim, J. Y.; Kim, S. H. J Polym Sci Part B: Polym Phys 2006, 44, 1062.
21. Kim, J. Y.; Han, S. I.; Kim, D. K.; Kim, S. H. Compos A 2009, 40, 45.
22. Kim, J. Y.; Kim, D. K.; Kim, S. H. Eur Polym J 2009, 45, 316.
23. Radusch, H. J. In Handbook of Thermoplastic Polyesters; Fakirov, S., Ed.; Wiley-VCH: Weinheim, 1993; Vol 1, chap. 8, pp 389–419.
24. Rubin, I. I. Handbook of Plastic Materials and Technology; Wiley: New York, 1990.
25. Tjong, S. C.; Meng, Y. Z. J Appl Polym Sci 1999, 74, 1827.
26. Kim, J. Y.; Kang, S. W.; Kim, S. H.; Kim, B. C.; Lee, J. G. Macromol Res 2005, 13, 19.
27. Kim, J. Y.; Kang, S. W.; Kim, S. H. Fibers Polym 2006, 7, 358.
28. Wu, D.; Wu, L.; Zhang, M. J Polym Sci Part B: Polym Phys 2007, 45, 2239.
29. Haggenmuller, R.; Conmas, H. H.; Rinzler, A. G.; Fischer, J. E.; Winey, K. I. Chem Phys Lett 2000, 330, 219.
30. Jin, J. X.; Pramoda, K. P.; Goh, S. H.; Xu, G. Q. Mater Res Bull 2002, 37, 271.
31. Pötschke, P.; Fornes, T. D.; Paul, D. R. Polymer 2002, 43, 3247.
32. Jung, R.; Park, W. I.; Kwon, S. M.; Kim, H. S.; Jin, H. J. Polymer 2008, 49, 2071.
33. Mu, M.; Walker, A. M.; Torkelson, J. M.; Winey, K. I. Polymer 2008, 49, 1332.
34. Pegel, S.; Pötschke, P.; Petzold, G.; Alig, I.; Dudkin, S. M. Polymer 2008, 49, 974.
35. Kim, J. Y.; Kim, S. H. Polym Int 2006, 55, 449.
36. Kim, J. Y.; Kim, S. H. J Polym Sci Part B: Polym Phys 2005, 43, 3600.
37. Kim, J. Y.; Kim, O. S.; Kim, S. H.; Jeon, H. Y. Polym Eng Sci 2004, 44, 395.
38. Kim, J. Y.; Kim, S. H. J Appl Polym Sci 2006, 99, 2211.
39. Kim, J. Y.; Kim, S. H.; Kikutani, T. J Polym Sci Part B: Polym Phys 2004, 42, 395.
40. Kim, J. Y.; Seo, E. S.; Kim, S. H.; Kikutani, T. Macromol Res 2003, 11, 62.
41. Song, Y. S.; Youn, J. R. Carbon 2005, 43, 1378.
42. Abdel-Goad, M.; Pötscke, P. J Non-Newtonian Fluid Mech 2005, 128, 2.
43. Costa, F. R.; Wagenknecht, U.; Jehnichen, D.; Abdel-Goad, M.; Heinrich, G. Polymer 2006, 47, 1649.
44. Krishnamoorti, R.; Giannelis, E. P. Chem Mater 1996, 8, 1728.
45. Krishnamoorti, R.; Giannelis, E. P. Macromolecules 1997, 30, 4097.
46. Ferry, J. Viscoelastic Properties of Polymers; Wiley: New York, 1980.
47. Rosedalev, J. H.; Bates, F. S. Macromolecules 1990, 23, 2329.
48. Larson, R. G.; Winey, K. I.; Patel, S. S.; Watanabe, H.; Bruinsma, R. Rheol Acta 1993, 32, 245.
49. Van Gulip, M.; Palmen, J. Rheol Bull 1998, 67, 5.
50. Han, C. D.; Kim, J.; Kim, J. K. Macromolecules 1989, 22, 383.
51. Ebbesen, T. Carbon Nanotubes: Preparation and Properties; CRC Press: New York, 1997.
52. Schadler, L. S.; Giannaris, S. C.; Ajayan, P. M. Appl Phys Lett 1998, 73, 3842.
53. Gorga, R. E.; Cohen, R. E. J Polym Sci Part B: Polym Phys 2004, 42, 2690.
54. Sepe, M. P. In Limitation of test methods for plastics, ASTM STP 1369; Petaro, J. S., Ed.; American Society for Testing and Materials: West Conshohocken, PA, 2000; pp 44–53.
55. Wong, A. C. Y. Compos B 2003, 34, 199.
56. Nielsen, L. E. Mechanical Properties of Polymers and Composites; Marcel Dekker: New York, 1974.
57. Thomasson, J. L.; Groenewoud, W. M. Compos A 1996, 27, 555.
58. Fakirov, S. Handbook of Thermoplastic Polyesters; Wiley-VCH: Weinheim, 1993.
59. Cheng, S. Z. D.; Wunderlich, B. Macromolecules 1988, 21, 789.
60. Nair, C. P. R.; Bindu, R. L.; Joseph, V. C. J Polym Sci Part A: Polym Chem 1995, 33, 621.
61. Vijayakumar, C. T.; Fink, J. K. Thermochim Acta 1982, 59, 51.
62. Kashiwagi, T.; Grulke, E.; Hilding, J.; Harris, R.; Awad, W.; Douglas, J. Macromol Rapid Commun 2002, 23, 761.
63. Park, S. J.; Cho, M. S. J Mater Sci 2000, 35, 3525.
64. Zanetti, M.; Camino, G.; Canavese, D.; Morgan, A. B.; Lamelas, F. G.; Wilkie, C. A. Chem Mater 2002, 14, 189.
65. Horowitz, H. H.; Metzger, G. Anal Chem 1963, 35, 1464.